

Chiral properties of light mesons in $N_f = 2 + 1$ overlap QCD

JLQCD and TWQCD collaborations: J. Noaki^{*,a†}, S. Aoki^{b,c}, T.W. Chiu^{d,c}, H. Fukaya^e, S. Hashimoto^{a,f}, T.H. Hsieh^g, T. Kaneko^{a,f}, H. Matsufuru^a, T. Onogi^h, E. Shintaniⁱ and N. Yamada^{a,f}

^a High Energy Accelerator Research Organization (KEK), Tsukuba 305-0801, Japan

^b Graduate School of Pure and Applied Sciences, University of Tsukuba, Tsukuba 305-8571, Japan

^c Center for computational Sciences, University of Tsukuba, Tsukuba, Ibaraki 305-8577, Japan

^d Physics Department, Center for Theoretical Sciences, and Center for Quantum Science and Engineering, National Taiwan University, Taipei 10617, Taiwan

^e Department of Physics, Nagoya University, Nagoya 464-8602, Japan

^f School of High Energy Accelerator Science, the Graduate University for Advanced Studies (Sokendai), Tsukuba 305-0801, Japan

^g Research Center for Applied Sciences, Academia Sinica, Taipei 115, Taiwan

^h Department of Physics, Osaka University Toyonaka, Osaka 560-0043, Japan

ⁱ Riken BNL Research Center, Brookhaven National Laboratory, Upton, NY 11973, USA

We summarize the project of the light meson spectrum with $N_f=2+1$ overlap fermions by the JLQCD and TWQCD collaborations. We study the finite size effect by comparing the analytical correction with the data on a larger volume lattice. Through the chiral extrapolation carried out using data points with the degenerate quark masses $m_{ud} = m_s$, we study the convergence property of chiral perturbation theory. With an increased number of data points and modified fit scheme, we update the results of the chiral extrapolation to obtain physical quantities.

The XXVIII International Symposium on Lattice Field Theory

June 14-19, 2010

Villasimius, Sardinia Italy

*Speaker.

†E-mail: noaki@post.kek.jp

1. Introduction

Since the chiral symmetry on the lattice is preserved by using the overlap fermions [1], dynamical simulations with this formalism enable us to study the continuum chiral perturbation theory (ChPT) including its dependence on N_f . In particular, it is important to examine the convergence property of ChPT using basic quantities such as the light meson masses and the decay constants to test the validity of the phenomenological studies around the kaon mass region ≈ 500 MeV. Along this direction, as an extension of our previous study for the $N_f = 2$ case [2], we generate gauge configurations with the $N_f = 2 + 1$ dynamical overlap fermions [3]. Preliminary results of the chiral extrapolation were presented in the last conference [4] with 5×2 combinations of the quark masses (m_{ud}, m_s) on a $16^3 \times 48$ lattice.

For the convergence study, the discussion can be made simpler by considering ChPT in the SU(3) limit with the degenerate quark masses $m_{ud} = m_s$. Since last year, we have added two more such simulations at the second and third lightest m_{ud} 's. On the other hand, because of high computational cost required for the overlap fermion, numerical simulations are performed on a small lattice, $16^3 \times 48$. Since the finite size effects (FSEs) could be significant in our work, we correct the data using the analytic formulae [5, 6]. In order to validate this step, we generate new gauge configurations on a larger volume, $24^3 \times 48$, at the two lightest m_{ud} 's and explicitly compare the data with the FSE correction formulae. In the following section, after explaining the profile of the data briefly, we discuss the finite volume effects on our data. A study on the convergence property of the SU(3) ChPT is given in Section 3. With the increased number of data points, in Section 4, we carry out the chiral extrapolation using the next-to-next-to-leading order (NNLO) ChPT and update the physical results.

2. Data profile and finite size effect

The details of the gauge configuration generation will be presented in a forthcoming paper which is under preparation [7]. In the data analysis, we first determine the lattice scale by the Ω -baryon mass. As shown in Figure 1, we fit all available data to the linear function $am_\Omega = M_0 + A(am_\pi)^2 + B(am_K)^2$ with $\chi^2/\text{dof} = 0.77$ and determine the parameters M_0 , A and B . From the input $m_\Omega = 1.672$ GeV, $m_\pi = 135$ MeV and $m_K = 495$ MeV, we obtain $a^{-1} = 1.759(8)(5)$ GeV, where the first error is statistical while the second contains systematic errors including the finite volume effect. Our data of the pion mass therefore cover the range 290–780 MeV.

Relevant observables m_π , m_K , f_π and f_K are computed by a simultaneous fit of the pseudo-scalar correlation functions with the local and the exponentially smeared sources. The renormalized decay constants are obtained by applying the axial-Ward-Takahashi identity to the amplitude of the pseudo-scalar correlator. In advance to the analysis, we compute a certain number of low-lying eigenvalues and eigenvectors on each gauge configuration and store on the disk; 80 (120) eigenpairs are computed in steps of 10 (100) trajectories for the simulations on the $16^3 \times 48$ ($24^3 \times 48$) lattice. Using these eigenmodes, we improve the statistical signal by averaging the contribution of the low-modes over various source locations in the temporal direction [8, 9]. As explained in [10], we calculate the renormalization factor of the quark mass $Z_m^{\overline{\text{MS}}}(\mu = 2 \text{ GeV})$ through the RI/MOM scheme on the lattice [11].

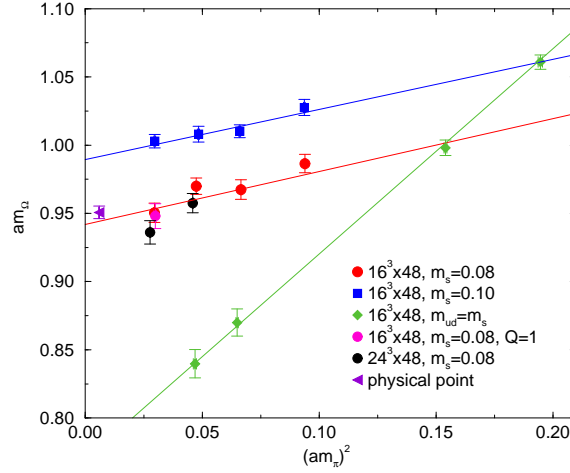


Figure 1: Plot of am_Ω from all gauge ensembles as a function of $(am_\pi)^2$.

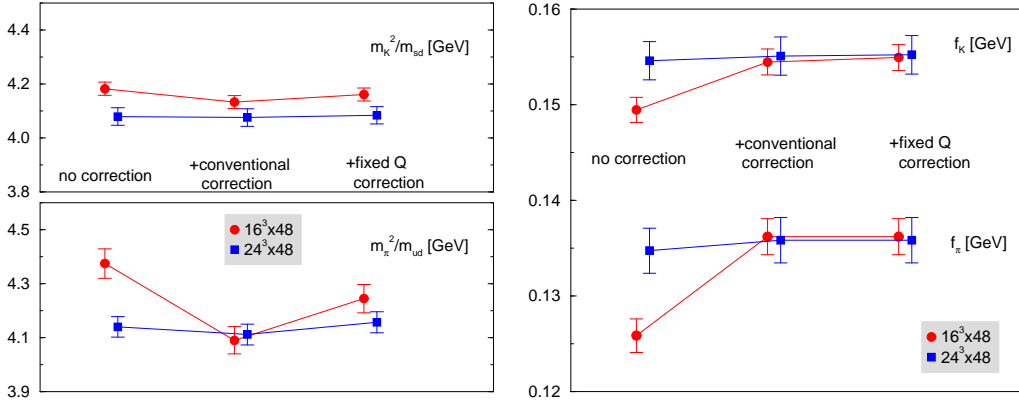


Figure 2: Transition of the data for the lightest quark mass by the finite size corrections. Left panels correspond to meson masses while the right shows the decay constants.

The conventional FSE caused by the pion wrapping around the spatial directions is analytically estimated in [5]. On top of that, since our gauge configurations are generated with a fixed topological charge, some deviation from the θ -vacuum is known to appear as another kind of finite volume effect [12, 13, 6]. The value of the topological susceptibility χ_t , which is needed for the correction, has already been calculated on the same ensembles in [14]. We therefore correct the data by a combination of the formulae for the two sources of FSE. In the case of the lightest m_{ud} , Figure 2 shows how much FSE corrections the original data of the meson masses m_π^2/m_{ud} and m_K^2/m_{sd} (left) and the decay constants f_π and f_K (right) receive on the different volumes $16^3 \times 48$ (circles) and $24^3 \times 48$ (squares). As expected from the values $m_\pi L = 2.75$ and 4.01 on these lattices, while all quantities in the smaller volume receive significant correction, the larger volume data remain stable against the corrections. (Note that f_π does not receive the fixed-topology correction at the leading order that we apply.) Between the fully corrected values in different volumes, we observe differences of at most 2σ . This remaining difference might be explained by higher order effects of the fixed-topology FSE. In order to include this effects, we have to reanalyze the correlators that may

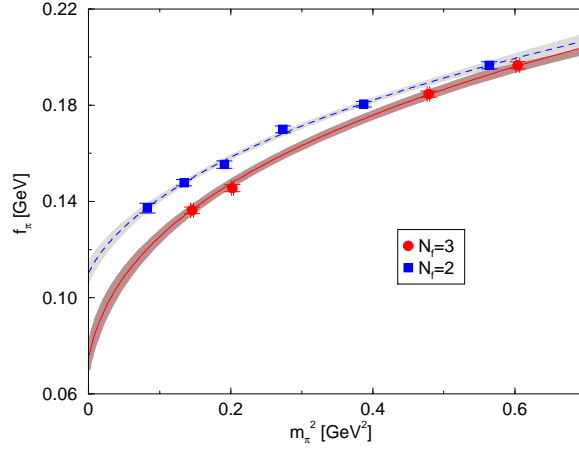


Figure 3: Plot of f_π for $N_f = 3$ (circles) and 2 (squares). Fit curves shown as an eye guide are obtained from the NNLO ChPT formulae.

have non-exponential functional form [6]. We take this difference into account in the systematic error of the final result.

In the following sections, it is understood that all observables are renormalized and FSE corrected so that they are directly comparable with the continuum ChPT.

3. Convergence of SU(3) ChPT

In the previous work for $N_f = 2$ [2], we found that the SU(2) ChPT calculation at NLO becomes questionable at around 500 MeV. To carry out the convergence study around this mass region, it is needed to employ the NNLO (or higher order) formulae. By the analogy of this observation, for the chiral extrapolation of the degenerate mass data, we employ the SU(3) NNLO formulae, which are given as

$$m_\pi^2/m_q = 2B_0 \left[1 + M_{\text{dg}}(\xi; L_1^r, L_2^r, L_3^r) - 8(4\pi)^2(3L_4^r + L_5^r)\xi \left(1 - \frac{25}{3}\xi \ln \xi \right) + 48(4\pi)^2 L_6^r \xi \left(1 - \frac{19}{3}\xi \ln \xi \right) + 16(4\pi)^2 L_8^r \xi \left(1 - 8\xi \ln \xi \right) \right] + \alpha \xi^2, \quad (3.1)$$

$$f_\pi = f_0 \left[1 + F_{\text{dg}}(\xi; L_1^r, L_2^r, L_3^r) + 4(4\pi)^2(3L_4^r + L_5^r)\xi \left(1 - \frac{15}{2}\xi \ln \xi \right) \right] + \beta \xi^2, \quad (3.2)$$

where the low-energy constants (LECs) L_i^r are renormalized at $\mu = 4\pi f_0$. Among them, L_1^r, L_2^r and L_3^r only appear in the two-loop terms in the non-analytic functions $M_{\text{dg}}(\xi)$ and $F_{\text{dg}}(\xi)$ [15]. For their values, we use the phenomenological estimates [16] as input: $L_1^r(m_\rho) = 0.43(12) \cdot 10^{-3}$, $L_2^r(m_\rho) = 0.73(12) \cdot 10^{-3}$ and $L_3^r(m_\rho) = -2.53(37) \cdot 10^{-3}$. Figure 3 compares the f_π data between $N_f = 2$ and 3. We note the difference of the curvature can be explained by the flavor dependence of the chiral log $F_{\text{dg}}(\xi) = N_f/2 \cdot \xi \ln \xi + \dots$.

From our experience in $N_f = 2$ QCD [2], the fit is expected to be numerically stabilized by using the expansion parameter $\xi = 2m_\pi^2/(4\pi f_\pi)^2$ which is constructed by the measured values. For the degenerate $N_f = 3$ case, due to the limited number of data points hence the small degree of freedom of the fit, there still remains large uncertainties. We therefore constrain the fit with a fixed

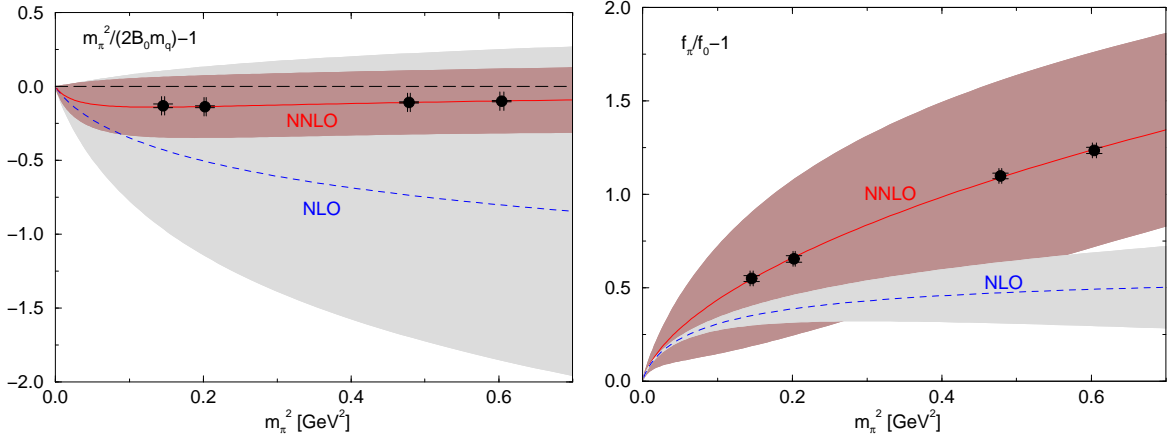


Figure 4: Result of the simultaneous fit to the NNLO ChPT prediction at the SU(3) limit for m_π^2/m_q (left) and f_π (right). Dashed curves represent mass dependence truncated at NLO.

Table 1: Convergence ratio of the chiral expansion for m_π^2/m_q and f_π at $m_q \simeq m_s/2$. As well as the $N_f = 2 + 1$ results, those from the $N_f = 2$ case are listed for comparison.

	m_π^2/m_q (NLO)	m_π^2/m_q (NNLO)	f_π (NLO)	f_π (NNLO)
$N_f = 2 + 1$	-56(71)%	+95(268)%	+41(29)%	+23.7(5.6)%
$N_f = 2$	-4.5(2.1)%	+1.91(63)%	+29.6(5.7)%	+16.0(1.0)%

value of the ratio $2B_0/f_0 = 54.76$ which is determined by an independent fit using all available data points to the non-degenerate SU(3) formulae (see Section 4). Taking the correlation between m_π and f_π on the same gauge ensemble into account, we carry out a simultaneous fit with $\chi^2/\text{dof} = 2.97$. We plot the deviations from the tree level values $m_\pi^2/(2B_0 m_q) - 1$ and $f_\pi/f_0 - 1$ respectively in the left and right panels of Figure 4. In the same figure, we draw curves truncated to NLO by using the same fit parameters. While the large jackknife errors represented by shades obscure the convergence property for m_π^2/m_q , we have a signal for f_π .

An important issue to be addressed here is the convergence property of the chiral expansion around $m_K \simeq 500$ MeV. In Table 1, we list the convergence ratio $(X_{\text{NLO}} - X_{\text{LO}})/X_{\text{LO}}$ and $(X_{\text{NNLO}} - X_{\text{NLO}})/X_{\text{NLO}}$, where X represents the value of m_π^2/m_q or f_π at $m_q \simeq m_s/2$. As expected from Figure 4, the large error for m_π^2/m_q does not allow for any solid conclusion. On the other hand, for f_π , we see the ratio decreasing from NLO to NNLO. This is a similar in magnitude to that in the $N_f = 2$ case [2] listed in the table for comparison.

4. Chiral extrapolation at NNLO

With increased data points explained in Section 2, we update the chiral extrapolation of the light meson observables using the NNLO ChPT formulae given as

$$m_\pi^2/m_{ud} = 2B_0 [1 + M^\pi(\xi_\pi, \xi_K; L_4^r, L_5^r, L_6^r, L_8^r)] + \alpha_1^\pi \cdot \xi_\pi^2 + \alpha_2^\pi \cdot \xi_\pi \xi_K + \alpha_3^\pi \cdot \xi_K^2, \quad (4.1)$$

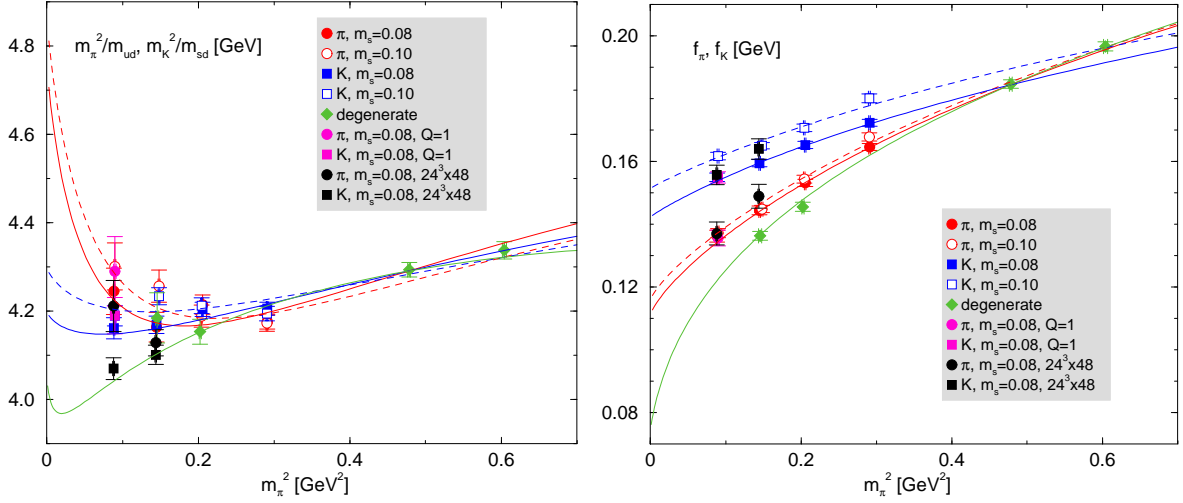


Figure 5: Chiral extrapolation of m_π^2/m_{ud} and m_K^2/m_{sd} (left panel) and f_π and f_K (right panel).

$$m_K^2/m_{sd} = 2B_0 [1 + M^K(\xi_\pi, \xi_K; L_4^r, L_5^r, L_6^r, L_8^r)] + \alpha_1^K \cdot \xi_\pi(\xi_\pi - \xi_K) + \alpha_2^K \cdot \xi_K(\xi_K - \xi_\pi), \quad (4.2)$$

$$f_\pi = f_0 [1 + F^\pi(\xi_\pi, \xi_K; L_4^r, L_5^r)] + \beta_1^\pi \cdot \xi_\pi^2 + \beta_2^\pi \cdot \xi_\pi \xi_K + \beta_3^\pi \cdot \xi_K^2, \quad (4.3)$$

$$f_K = f_0 [1 + F^K(\xi_\pi, \xi_K; L_4^r, L_5^r)] + \beta_1^K \cdot \xi_\pi(\xi_\pi - \xi_K) + \beta_2^K \cdot \xi_K(\xi_K - \xi_\pi), \quad (4.4)$$

where there are two expansion parameters defined as $\xi_\pi = 2m_\pi^2/(4\pi f_\pi)^2$ and $\xi_K = 2m_K^2/(4\pi f_K)^2$. Non-analytic functions M^π , M^K , F^π and F^K represent the loop corrections to the two-loop level [15].

By a simultaneous correlated fit, we obtain fit curves shown in Figure 5 with $\chi^2/\text{dof}=2.6(1.0)$. Besides increased data points, we modify the fit scheme so that the fit is done for fixed values of $2B_0/f_0$. Then we minimize χ^2 by varying the input value for this ratio. By this simplification, the fit formulae (4.1)–(4.4) become a set of linear functions of unknown parameters. We further approximate the formulae by setting $\alpha_3^\pi = \beta_3^\pi = 0$ to drop the ξ_K^2 terms which cannot be distinguished from other analytic terms with our data. As seen in the formulae by the partially-quenched ChPT [17], this is amount to dropping the dependence on the sea-strange quark mass squared in the NNLO analytic terms. No significant effect from this approximation is observed in the fit results which are consistent with the independent fit in previous section.

Because of the degenerate mass point, we obtain more stable fit results for SU(3) LECs than before. The pre-final results are

$$f_0 = 74.0(6.6) \text{ MeV}, \quad \Sigma_0^{1/3} \equiv (f_0 B_0/2)^{1/3} = 177(12) \text{ MeV}, \quad (4.5)$$

$$L_4^r(m_\rho) = 8.2(3.4) \cdot 10^{-4}, \quad L_5^r(m_\rho) = -8.0(6.7) \cdot 10^{-4}, \quad (4.6)$$

$$L_6^r(m_\rho) = 3.5(2.5) \cdot 10^{-4}, \quad L_8^r(m_\rho) = -3.2(3.0) \cdot 10^{-4}. \quad (4.7)$$

Our result of f_0 is substantially smaller than the phenomenological estimate $f_0 = 124 \text{ MeV}$ [16]. As mentioned in the previous section, the N_f dependence of our data can be described by ChPT. Therefore, it is inevitable for f_0 to be significantly smaller than the SU(2) LEC $f \simeq 110 \text{ MeV}$, which is obtained in [2]. Also, there is a large difference between $\Sigma_0^{1/3}$ and the SU(2) chiral condensate $\Sigma^{1/3} \simeq 230 \text{ MeV}$ [2].

By the extrapolation to the physical point $(m_\pi, m_K) = (135 \text{ MeV}, 495 \text{ MeV})$, we extract physical values of the decay constants. Also, from the ratio of the physical pion mass (kaon mass) and the extrapolated values of m_π^2/m_{ud} (m_K^2/m_{sd}), we obtain physical quark masses m_{ud} and m_s . The results with the jackknife error estimate are

$$f_\pi = 118.5(3.6) \text{ MeV}, \quad f_K = 145.8(2.7) \text{ MeV}, \quad f_K/f_\pi = 1.230(19), \quad (4.8)$$

$$m_{ud} = 4.028(57) \text{ MeV}, \quad m_s = 113.4(1.2) \text{ MeV}, \quad m_s/m_{ud} = 28.15(23). \quad (4.9)$$

There are also systematic errors originating from the FSE correction, the determination of the lattice scale and the quark mass renormalization. Errors in the input LECs values have to be considered, as well. More discussions and studies about these issues will be presented in [7].

Numerical simulations are performed on Hitachi SR11000 and IBM System Blue Gene Solution at High Energy Accelerator Research Organization (KEK) under a support of its Large Scale Simulation Program (No. 09/10-09). This work is supported in part by the Grant-in-Aid of the Ministry of Education (Nos. 20105001, 20105002, 20105003, 20105005, 20340047, 21105508, 21674002, 21684013, 220340047) and the National Science Council of Taiwan (Nos. NSC99-2112-M-002-012-MY3, NSC99-2112-M-001-017-MY3, NSC99-2119-M-002-001), and NTU-CQSE (Nos. 99R80869, 99R80873).

References

- [1] H. Neuberger, Phys. Lett. **B427** (1998) 353
- [2] JLQCD and TWQCD Collaborations (J. Noaki *et al.*), Phys. Rev. Lett. **101** (2008) 202004. The updated results will appear in [7].
- [3] JLQCD and TWQCD Collaborations (H. Matsufuru *et al.*), PoS **LAT2008** (2008) 077.
- [4] JLQCD and TWQCD Collaborations (J. Noaki *et al.*), PoS **LAT2009** (2009) 096.
- [5] G. Colangelo, S. Dürr and C. Haefeli, Nucl. Phys. **B721** (2005) 136.
- [6] S. Aoki and H. Fukaya, Phys. Rev. D **81** (2010) 034022.
- [7] JLQCD and TWQCD Collaborations, under progress.
- [8] T. DeGrand and S. Schaefer, Comp. Phys. Comm. **159** (2004) 185.
- [9] L. Giusti, P. Hernández, M. Laine, P. Weisz, H. Wittig, JHEP **04** (2004) 013.
- [10] JLQCD and TWQCD Collaborations (J. Noaki *et al.*), Phys. Rev. D **81** (2010) 034502.
- [11] G. Martinelli, C. Pittori, C. T. Sachrajda, M. Testa and A. Vladikas, Nucl. Phys. **B445** (1995) 81.
- [12] R. Brower, S. Chandrasekharan, J. W. Negele and U.-J. Wiese, Phys. Lett. **B560** (2003) 64.
- [13] S. Aoki, H. Fukaya, S. Hashimoto and T. Onogi, Phys. Rev. D **76** (2007) 054508.
- [14] JLQCD and TWQCD Collaborations (T.H. Hsieh *et al.*), PoS (**LATTICE 2009**) (2009) 085.
- [15] G. Amorós, J. Bijnens and P. Talavera, Nucl. Phys. **B568** (2000) 319. We thank J. Bijnens for providing his FORTRAN code evaluating the contribution of sunset integrals among the two-loop effects.
- [16] J. Bijnens, PoS (**LATTICE 2007**) (2007) 004.
- [17] J. Bijnens and T. Lähde, Phys. Rev. D **72** (2005) 074502.